Langmuir

Article

pubs.acs.org/Langmuir

Reduced Condensing and Ordering Effects by 7-Ketocholesterol and 5β,6β-Epoxycholesterol on DPPC Monolayers

Dana-Marie Telesford, Dominique Verreault, Victoria Reick-Mitrisin, and Heather C. Allen*

Department of Chemistry & Biochemistry, The Ohio State University, 100 West 18th Avenue, Columbus, Ohio 43210, United States

Supporting Information

ABSTRACT: The exposure of organic-coated marine aerosols containing cholesterol (Chol) to radiation and/or an oxidizing atmosphere results in the formation of oxidized derivatives or oxysterols and will likely change aerosol surface properties. However, the intermolecular interactions between oxysterols and other lipid components and their influence on the surface properties of marine aerosols are not well-known. To address this question, the interfacial behavior and domain morphology of model Langmuir monolayers of two ring-substituted oxysterols, 7-ketocholesterol (7-KChol) and 5β,6β-epoxycholesterol (5,6β-EChol), mixed with 1,2-dipalmitoyl-*sn*-glycero-3-phosphocholine (DPPC) were investigated by means of compression isotherms and Brewster angle microscopy (BAM) over a broad range of surface pressures and sterol molar ratios. Mixed DPPC/cholesterol (Chol) monolayers were also measured for comparison. The results of compression experiments showed that the condensing effect induced on mixed DPPC/sterol monolayers at low surface pressures and for intermediate molar ratios ($0.3 \leq X_{sterol} \leq 0.7$) was weaker for oxysterols than for Chol. Additionally, mixed DPPC/oxysterol monolayers exhibited markedly smaller (~2−3-fold) interfacial rigidity. Examination of the excess free energy of mixing further revealed that DPPC monolayers containing 7-KChol and Chol were thermodynamically more stable at high surface pressures than those with 5,6β-EChol, indicating that the strength of interactions between DPPC and 5,6β-EChol was the smallest. Finally, BAM images in the LE−LC phase of DPPC revealed that in comparison to Chol the addition of small amounts of oxysterols results in larger and less numerous domains, showing that oxysterols are not as effective in fluidizing the condensed phase of DPPC. Taken together, these results suggest that the strength of van der Waals interactions of DPPC alkyl chains with sterols follows the sterol hydrophobicity, with Chol being the most hydrophobic and oxysterols more hydrophilic due to their ketone and epoxy moieties. The difference in the condensing ability and stability of 7-KChol and 5,6β-EChol on DPPC likely originates from the distinct molecular structure and position of oxidation on the steroid nucleus. As suggested by recent MD simulations, depending on the oxidation position, ring-substituted oxysterols have a broader angular distribution of orientation than Chol in bilayers, which could be responsible for the observed reduction in condensing ability.

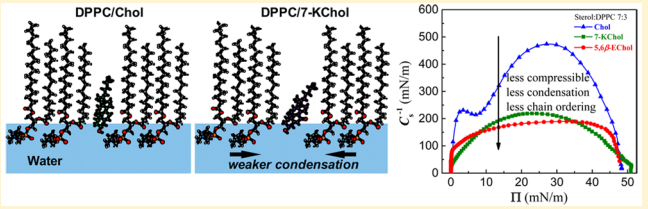

INTRODUCTION

Given the vastness of the oceans, marine aerosols constitute one of the most important and largest reservoir of atmospheric aerosols on a global scale.[1] Marine aerosols have garnered much interest because they play a critical role in atmospheric chemistry, in the biogeochemical cycling of nutrients (e.g., C, N, and S), and in global climate change through their effect on cloud condensation nuclei, radiative balance, and levels of precipitation.[2] Primary marine organic aerosols originate mainly from wind-driven turbulent wave action at the ocean surface, more specifically through the production of sea spray from bubble bursting and liquid jets.[1,3,4] Through this process, newly formed marine aerosols become enriched in organic matter found in the sea surface microlayer (SSML), the thin (1−1000 μm) organic layer present at the ocean's surface.[5,6]

The organic matter present in the SSML and on marine aerosols is a complex mixture mainly composed of various lipid components found in the biomembranes of living and decaying marine microorganisms (bacteria, plankton) that have risen to the sea surface. These components include, among others, free fatty acids, phospholipids, sphingolipids, and sterols. Phospholipids, because of their prevalence in marine cellular membranes, exist in some abundance in the SSML,[7] predominantly phosphatidylcholines (PC) with C_{14} to C_{18} saturated alkyl chains like dipalmitoylphosphatidylcholine (DPPC).[8] Sterols, another prominent component of cellular membranes of marine origin, have also been found in the SSML.[9,10] Among the sterols, cholesterol (Chol) is the most abundant at the marine surface.[11] Because of their amphiphilic character, molecules like DPPC and Chol are surface-active, i.e., readily adsorb at the ocean and aerosol surfaces to form mixed monolayers. For instance, there is evidence that marine aerosols adopt a structure resembling that of "inverted micelles", i.e., an aqueous salty core surrounded by a monolayer of surface-active organic components with their hydrophobic chains exposed to the atmosphere.[12−15] Because of its molecular structure, Chol is

Received: July 14, 2015
Revised: August 28, 2015
Published: August 31, 2015

DOI: 10.1021/acs.langmuir.5b02539
Langmuir 2015, 31, 9859−9869

likely to affect the molecular organization and phase behavior of other lipid components, thus modifying the surface properties of marine aerosols and influencing their atmospheric processing and reactivity. For example, model monolayer studies of Chol mixed with DPPC and other saturated PCs have shown that Chol promotes the orientational ordering of phospholipid alkyl chains, thereby leading to a tighter packing density of the phospholipids, a phenomenon referred to as the "condensing effect".[16−18] This has the consequence of increasing the mechanical strength and decreasing the permeability of the monolayer. Both condensing and ordering effects attributed to Chol are highly dependent upon its molecular structure.

While Chol is relatively stable, its long-term exposure to gas-phase free radicals and oxidants, solar radiation, and/or heat leads to the formation of oxidized derivatives or oxysterols.[19] Oxysterols typically involve the substitution on Chol's steroid nucleus (A−D rings) of an additional oxygen atom in the form of a ketone, hydroxyl, hydroperoxy, or epoxy group.[20] Two common ring-substituted oxysterols formed through this oxidative pathway are 7-ketocholesterol (7-KChol) and 5β,6β-epoxycholesterol (5,6β-EChol) (Figure 1). The molecular

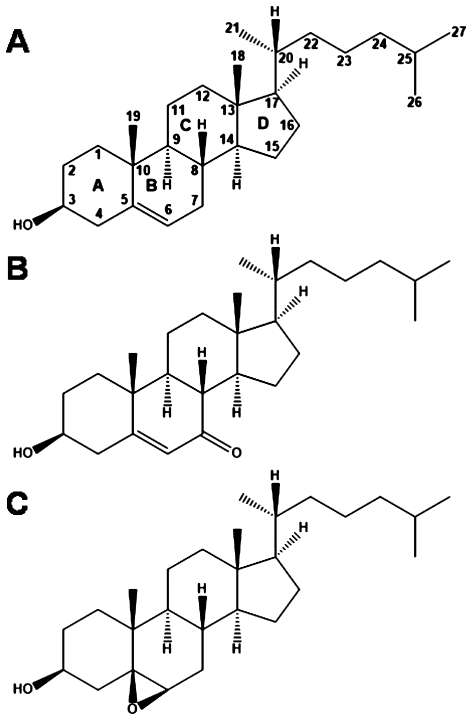

Figure 1. Chemical structures of (A) Chol, (B) 7-KChol, and (C) 5,6β-EChol.

structure of 7-KChol differs from Chol with respect to the additional ketone group at C7 on the steroid nucleus. 5,6β-EChol differs in that there is no double bond between C5 and C6 and also by the presence of an epoxy group that projects out of the β-face of the steroid nucleus, i.e., the face on which the two methyl groups at C10 and C13 are located. In addition, the absence of the double bond between C5 and C6 destroys the planarity of the Chol's A and B rings.[21] Of the two oxysterols, only 5,6β-EChol has so far been detected as a Chol degradation product in arctic waters.[9]

On the basis of the chemical and structural differences of oxysterols relative to Chol, one might expect that their presence may alter the surface properties and morphology of the organic layer and, in turn, impact the processing and reactivity of the marine aerosol. Thus, a fundamental understanding of the surface properties including intermolecular interactions and molecular organization of oxysterols on model systems of marine aerosols is highly desirable.[22] One proven experimental approach is to use Langmuir monolayers of simple mixtures of pure lipid and sterol components on an aqueous salt solutions as simplified model systems in which the chemical composition and other environmental parameters can be easily varied.[23] Although there are numerous studies on mixed PC/sterol monolayers using various experimental techniques, most have been concerned with nonoxidized Chol derivatives. To date, there are only a few theoretical and even fewer experimental published studies on mixed PC/oxysterol monolayers.[24−27] For instance, the relationship between the oxidation position on oxysterols, and their condensing and ordering effects on PC monolayers remain largely unexplored.[28−30]

Hence, to understand oxysterol interactions with other lipids components relative to Chol and to assess their potential impact on marine aerosols, the interfacial behavior and surface morphology of mixed Langmuir monolayers of 7-KChol and 5,6β-EChol (as well as Chol as a comparison) with DPPC, a model lipid commonly found in the organic layer of marine aerosols, are studied using compression isotherms and Brewster angle microscopy over a broad range of surface pressures and sterol molar ratios. The broad range of surface pressures used in this study is quite important because it can provide conclusive information regarding the physical state of the monolayer and the intermolecular interactions between dissimilar lipid components. We show that 7-KChol and 5,6β-EChol have reduced condensing and ordering capabilities on DPPC compared to Chol. This inability or poor performance varies with the chemical composition and the physical state of the mixed monolayers. To our knowledge, this is the first study comparing the interactions between these two ring-oxidized oxysterols and a commonly occurring saturated phospholipid (DPPC) and assessing their influence on the phase behavior of the mixed monolayers. Furthermore, the differences revealed here with the oxysterols underscore the importance of the oxidation substitution position in determining the oxysterol hydrophobic character and orientation in the host monolayer. The results presented here may be of significance to marine aerosols exposed to an oxidizing atmosphere as the occurrence of oxysterols likely change the chemical, mechanical, and optical properties of the organic layer which, in turn, may affect their growth, processing, and reactivity.

MATERIALS AND METHODS

Materials. 1,2-Dipalmitoyl-*sn*-glycero-3-phosphocholine (DPPC, >99%), 7-ketocholesterol (7-KChol, >99%), and 5β,6β-epoxycholesterol (5,6β-EChol, >99%) were purchased from Avanti Polar Lipids (Alabaster, AL), whereas cholesterol (Chol, >99%) was from Sigma-Aldrich (St. Louis, MO). All compounds were used without further purification. 1 mM DPPC and sterol stock solutions were prepared in chloroform (HPLC grade, ≥99.0%, Fisher Scientific, Pittsburgh, PA). Mixed DPPC/sterol solutions with the desired molar ratio were prepared from these stock solutions. Fresh ultrapure Milli-Q water with a resistivity of 18.2−18.3 MΩ·cm and a measured pH of 5.6 (the pH is slightly acidic due to the dissolution of atmospheric CO_2) was obtained from a Barnstead Nanopure system (model D4741, Barnstead/Thermolyne Corporation, Dubuque, IA) equipped with additional organic removing cartridges (D5026 Type I ORGANICfree Cartridge Kit; Pretreat Feed) and was used as subphase in all monolayer experiments.

DOI: 10.1021/acs.langmuir.5b02539
Langmuir 2015, 31, 9859−9869

Methods. Compression Isotherm Measurements. Surface pressure−molecular area (Π−A) compression isotherms were measured on a computer-controlled Langmuir film balance system (KSV Minitrough, Biolin Scientific, Linthicum Heights, MD). The Teflon-coated Langmuir trough (KN1001, A_{total} = 150 cm^2) has two Delrin-coated barriers for symmetrical monolayer compression. The trough was placed on a vibration-isolated optical table at the center of a Brewster angle microscope setup (see below). The combined setup was enclosed in a black Plexiglas box to limit ambient air currents, dust particles, and parasitic light. A defined volume of pure or mixed lipidic solution was spread dropwise onto the water subphase using a 50 μL glass microsyringe (model 705, Hamilton, Reno, NV) with the trough barriers initially in the fully expanded position. The spreading solvent was then allowed to evaporate for at least 10 min, after which the monolayer was symmetrically compressed at a speed of 6 Å^2/(molecule min). This compression rate was slow enough to limit unwanted domain growth artifacts coming from diffusion-limited aggregation.[31] Surface pressure was monitored during compression using a filter paper (Ashless Whatman 41, Sigma-Aldrich) Wilhelmy plate hung to the surface pressure sensor. The surface pressure is defined as[32]

$$\Pi = \gamma_0 - \gamma \quad (1)$$

where γ_0 and γ are the surface tensions of the bare and monolayer-covered air/water interfaces, respectively. Monolayer data were collected using Biolin Scientific proprietary software and analyzed using OriginPro (v. 9.0, OriginLab, Northampton, MA).

All isotherms were recorded at room temperature (21 ± 1 °C) in a climate-controlled environment and were repeated at least three times to ensure reproducibility. The standard deviations of the measured mean molecular area (MMA) and surface pressure were ±0.5 Å^2/molecule and ±1 mN/m, respectively. To address monolayer stability, each compression isotherm was completed within approximately 30 min, as a significant onset of oxidation of pure Chol monolayers is known to occur around 45 min after spreading.[25] Similarly, oxidation of Chol mixed in DMPC monolayers was shown to be detectable only after 40 min of air exposure.[33]

Isotherm Analysis. The change in the monolayer rigidity due to the ordering effect of sterols on DPPC alkyl chains was analyzed using the isothermal compressibility modulus (C_s^{-1}) calculated from the compression isotherm data following[32]

$$C_s^{-1} = -A_\Pi(\mathrm{d}\Pi/\mathrm{d}A)_T \quad (2)$$

where A_Π is the MMA at a given surface pressure Π. Large C_s^{-1} values correspond to a higher interfacial (in-plane) rigidity and more ordered alkyl chains.[34]

Intermolecular interactions between DPPC and sterols in the mixed monolayers were analyzed with the help of the excess free energy of mixing (ΔG_{exc}) as a function of sterol composition, which corresponds to the compression work difference between the real and ideal mixtures. It was calculated from the experimental compression isotherm data following[32,35]

$$\Delta G_{exc} = N_A \int_0^\Pi \Delta A_{exc}\, \mathrm{d}\Pi \quad (3)$$

where the excess MMA (ΔA_{exc}) for the mixed monolayer at a given pressure Π corresponds to the difference between the experimental MMA (A_{12}) measured from the compression isotherm and the ideal MMA (A_{12}^{id}) calculated from the additivity rule:[32,36]

$$\Delta A_{exc} = A_{12} - A_{12}^{id} = A_{12} - [(A_1)_\Pi X_1 + (A_2)_\Pi X_2] \quad (4)$$

where A_1 and A_2 are the MMAs of the pure components 1 and 2, respectively, X_1 and X_2 (= 1 − X_1) are their corresponding mole fractions, and N_A is Avogadro's constant. Negative or positive ΔG_{exc} deviations are an indication of nonideal behavior, with negative and positive values implying cohesive interactions between dissimilar (DPPC and sterol) and/or similar (DPPC−DPPC or sterol−sterol) components. Errors for the excess surface area (<±1 Å^2) and the excess free energy of mixing (<±0.05 kJ/mol) values were calculated and found to be negligible.

Brewster Angle Microscopy (BAM). Microscopic images of the monolayer domain morphology were obtained with a custom-built Brewster angle microscope equipped with a 5 mW He−Ne laser source (Research Electro-Optics, Boulder, CO) emitting a p-polarized (>500:1) light beam at a wavelength of 543 nm. The output beam is first attenuated by a neutral density filter and then passed through a half-wave plate and a Glan-Laser calcite polarizer (GL10-A, extinction ratio 100000:1; Thorlabs, Newton, NJ) before reaching the aqueous surface at the Brewster angle ($\theta_B \approx 53.1°$). The reflected light beam is then collected by a 10× infinity-corrected microscope objective (CFI 60 TU Plan EPI, NA 0.35; Nikon, Melville, NY) coupled to a lens tube and finally directed to an air-cooled, back-illuminated EM-CCD camera (DV887-BV, 512 × 512 pixels with 24 μm × 24 μm pixel size; Andor Technology, South Windsor, CT). Images were acquired with the Andor Solis software (v. 4.15.30000.0, Andor Technology). A blue background was selected to enhance image contrast. Because the focal plane of the microscope objective does not coincide with the aqueous surface due to the optics inclination, only a small strip in the central portion of the image can be in focus. The images were therefore cropped from the original 800 μm × 800 μm size to show the most resolved region. The lateral resolution of the BAM images was ∼2.2 μm. BAM measurements are based on the change caused by the presence of a spread monolayer of thickness d on the near-zero reflectance of p-polarized light at the Brewster angle on the neat air/water interface. The reflectance change is given by

$$\Delta R = R(0) - R(d) = R_0 - R \quad (5)$$

where R_0 and R are the reflectances of the bare and monolayer-covered air/water interfaces, respectively. Even for thin films, this difference is very large and can thus be used as an imaging contrast.

RESULTS AND DISCUSSION

Surface Pressure−Area Compression Isotherms of Pure Sterol Monolayers. The compression isotherms of the pure sterol monolayers are shown in Figure 2. Chol, 7-KChol, and 5,6β-EChol have lift-off areas (A_{lo}) of ∼37, ∼39.5, and ∼39 Å^2/molecule, respectively (Table 1). With respect to Chol and 7-KChol, A_{lo} values are in agreement with previously published data; however, it is also important to note that small differences do exist in the literature due to the different experimental conditions, for instance, temperature and compression rate.[30,37,38] The small area increase associated with the oxysterols is likely due to the more pronounced steric hindrance and electrostatic repulsion between neighboring

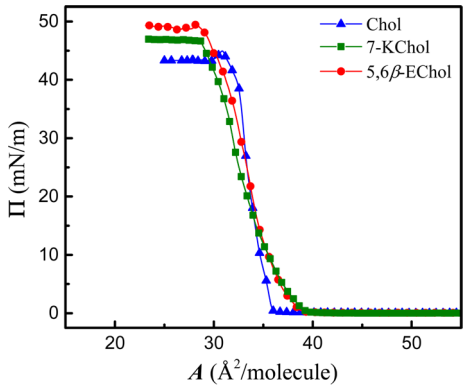

Figure 2. Compression isotherms of pure Chol, 7-KChol, and 5,6β-EChol monolayers. The pure oxysterols films exhibit high stability upon collapse, with the pure 5,6β-EChol monolayer being the most stable of the three, reaching a collapse pressure of ∼50 mN/m.

DOI: 10.1021/acs.langmuir.5b02539
Langmuir 2015, 31, 9859−9869

Table 1. Interfacial Properties of Pure Sterol Monolayers[a]

sterol	A_{lo} (Å^2/molecule)	A_0 (Å^2/molecule)	A_c (Å^2/molecule)	Π_c (mN/m)
Chol	37	37	32	45.0
7-KChol	39.5	39.5	28.5	46.7
5,6β-EChol	39	39	28.5	49.5

[a]Legend: A_{lo}, lift-off area; A_0, limiting area at zero surface pressure; A_c, collapse area; Π_c, collapse surface pressure.

molecules caused by the additional ketone and epoxy moieties. In addition, both oxysterol isotherms display a more gradual increase in surface pressure after lift-off in comparison to Chol, which is indicative of more disordered monolayers. It was previously suggested that the disorder of 7-KChol monolayers is likely caused by the marked change in tilt orientation of the oxysterol molecules.[30,39]

Another interesting feature in the isotherms is the slightly higher collapse surface pressures (Π_c) reached by 7-KChol and 5,6β-EChol (46.7 and 49.5 mN/m) relative to Chol (45.0 mN/m). This result suggests that the additional oxygen atom, whether it be a ketone or epoxide on the B ring, has some impact on the pure oxysterol monolayer stability upon collapse, with the pure 5,6β-EChol monolayer being the most stable. By closer inspection of Figure 2, a spike in surface pressure is also observed at the collapse of Chol and 5,6β-EChol but not for 7-KChol. The collapse of Chol and 5,6β-EChol monolayers therefore appears to undergo a similar collapse process: first, the surface pressure reaches a maximum, and then it slightly decreases before stabilizing in the form of a long plateau region. However, by comparison, the postcollapse pressure decrease is mostly prominent in the Chol monolayer followed by the 5,6β-EChol monolayer but barely noticeable for 7-KChol. Previous work on the collapse of Chol monolayers has attributed this surface pressure drop to the initial formation of an unstable 3D phase (aggregates) within the 2D monolayer that rapidly transforms into another more stable 3D collapse phase and reaches equilibrium with the monolayer at a slightly lower surface pressure.[40] Because of the similarities in the collapse onset with Chol and 5,6β-EChol isotherms, a similar aggregation mechanism may also be involved.

Surface Pressure−Area Compression Isotherms of Mixed DPPC/Sterols Monolayers. The influence of sterol type and composition on the phase behavior of DPPC was investigated by comparing representative compression isotherms of DPPC monolayers mixed with Chol, 7-KChol, and 5,6β-EChol (Figure 3). For the pure DPPC monolayer, the compression isotherm shows a typical liquid expanded−liquid condensed (LE−LC) coexistence plateau region at surface pressures between ∼3.5 and 6 mN/m, in agreement with previously published isotherms.[41,42] It is important to note that at the temperature used the true collapse pressure of DPPC should be found near 70 mN/m.[43] However, with the Langmuir trough used here, such high surface pressures could not be reached because of film leakage induced by subphase surface meniscus inversion.[44] For this reason, the thermodynamic analysis developed below will be restricted to low to moderate surface pressure ranges ($\Pi \leq 40$ mN/m).

In contrast to pure DPPC monolayer, the addition of sterols has a profound effect on the compression isotherms (Figure 3). In particular, one can see that with the increase of the sterol molar ratio (X_{sterol}) the LE−LC coexistence region progressively shifts to lower MMAs and narrows until it completely

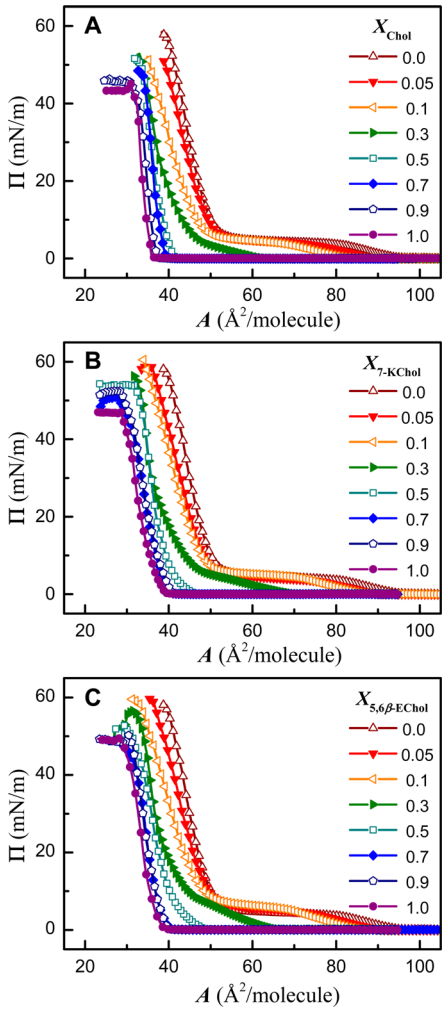

Figure 3. Compression isotherms of (A) Chol, (B) 7-KChol, and (C) 5,6β-EChol mixed with DPPC monolayers.

disappears ($X_{sterol} > 0.3$). This effect has to do with the increased van der Waals interactions between the DPPC alkyl chains and the sterol rings. Moreover, this phase transition occurs at different surface pressures for each sterol. For example, for $X_{Chol} = 0.1$, the LE−LC coexistence region is found at a slightly lower surface pressure in comparison to pure DPPC, whereas with the oxysterols, the small but opposing trend is observed.

The impact of the increasing sterol concentration on the DPPC isotherm is also reflected by the progressive decrease of its lift-off area. For instance, the lift-off area of the pure DPPC monolayer is ∼97 Å^2/molecule; however, for X_{Chol} ranging from 0.05 to 0.5, the lift-off area is reduced from ∼90 to 42 Å^2/molecule. In the case of 7-KChol and 5,6β-EChol, the lift-off areas are also reduced, although to a lesser extent, going from ∼90 to 47 Å^2/molecule over the same molar ratio range. Prior studies of DPPC monolayers mixed with Chol and other Chol derivatives have reported a similar reduction of the DPPC lift-off area with increasing sterol concentration, a phenomenon commonly referred to as the "condensing effect".[45,46] The results shown here clearly indicate that oxysterols are capable of condensing DPPC, yet to a lesser extent than Chol. For the same molar ratio, the sterol condensing effect follows the trend Chol > 5,6β-EChol > 7-KChol, a trend that correlates well with the sterol hydrophobic character. Various mechanisms have

DOI: 10.1021/acs.langmuir.5b02539
Langmuir 2015, 31, 9859−9869

been proposed to explain the condensing effect, the two most widely accepted being the stable complex formation and, more recently, the "umbrella effect".[47,48] In the stable complex formation, the condensing effect results from attractive van der Waals interactions between the phospholipid alkyl chains and the sterol rings in the binary mixture, whereas with the umbrella effect the phospholipid headgroups are believed to protect the hydrophobic part of the sterol from the aqueous subphase, thereby favoring closer proximity. Here, the observed trend would suggest that the strength of van der Waals interactions with DPPC follow the sterol hydrophobicity, with Chol being the most hydrophobic and oxysterols more hydrophilic due to their ketone and epoxy moieties.

To understand the impact of the physical state of the mixed monolayer on the condensing effect, the variation (using eq 4) of MMA as a function of sterol composition was analyzed for different constant surface pressures (see Figure S1 in the Supporting Information). Based on the magnitude of the (negative) deviation from the additivity rule, it is evident that the condensing effect is more effective in the LE phase (~3 mN/m) for all mixed DPPC/sterol monolayers. At higher surface pressures (≥10 mN/m), the condensing effect is significantly reduced because DPPC is already in a more condensed state. Overall, in the low and high surface pressure regimes, mixed monolayers with a sterol composition in the range $0.3 \leq X_{sterol} \leq 0.7$ showed the greatest condensing. Additionally, the condensing effect also shows some dependency on the sterol type. For example, at low surface pressures (e.g., 3 mN/m), mixed DPPC/sterol monolayers in the range $0.3 \leq X_{sterol} \leq 0.7$ follow the order Chol > 7-KChol > 5,6β-EChol, with Chol having the strongest condensing ability and 5,6β-EChol the weakest. In this pressure regime, the chemical type, hydrophobicity character, molecular structure, and possibly also the orientation of the sterols could play a role in dictating the condensing effect. Even with a comparable hydrophilicity, the condensing ability of 7-KChol and 5,6β-EChol likely differs based on their distinct molecular structure (planar vs nonplanar steroid nucleus) and tilted orientation in the DPPC monolayers. In contrast, at 40 mN/m these factors become less important as any of these sterols achieve a reduced but similar DPPC condensing. Overall, the extent of the condensing ability is dependent on the concentration, sterol type, and the physical state of the monolayer.

Interfacial Compressibility Modulus of Pure and Mixed DPPC/Sterol Monolayers. To gain further insight into the physical state of the mixed monolayers, the change of the isothermal compressibility modulus (C_s^{-1}) calculated from the compression isotherms was analyzed as a function of surface pressure and sterol composition (Figure 4A–C). By comparison, pure 5,6β-EChol (248 mN/m) and 7-KChol (223 mN/m) monolayers possess much smaller compressibility moduli than Chol (620 mN/m). According to Davies and Rideal, C_s^{-1} values in the range of 100–250 mN/m are indicative of a monolayer in the LC phase, while larger values reveal that the monolayer is in a solid state with closely packed alkyl chains.[49]

The impact of the sterols on DPPC phase behavior and chain ordering is also reflected by the interfacial compressibility modulus.[46,50] A phase transition is typically observed as a dip in the compressibility curve. The pure DPPC and mixed DPPC/sterol monolayers with $X_{sterol} \leq 0.1$ show similar interfacial rigidity as the LE–LC phase transition is still observed between 3.5 and 10 mN/m (indicated by an arrow in Figure 4). In the

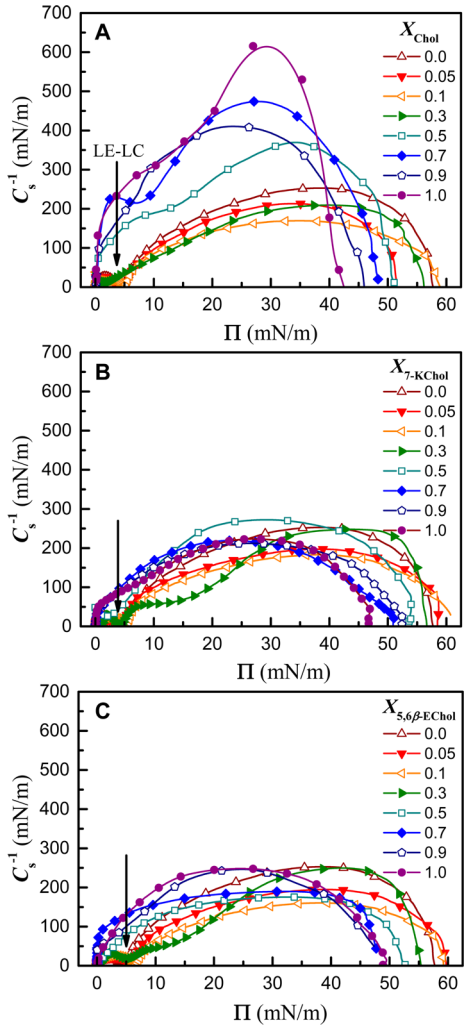

Figure 4. Variations of monolayer compressibility modulus with surface pressure for (A) Chol, (B) 7-KChol, and (C) 5,6β-EChol mixed with DPPC monolayers. The compressibility data were calculated from the compression isotherms in Figure 3. The position of the LE–LC phase transition in the compressibility curves is indicated by an arrow. A larger compressibility modulus correlates with higher rigidity of the monolayer.

DPPC/Chol monolayer with $X_{Chol} \leq 0.1$, the LE–LC coexistence region appears to overlap with that of pure DPPC. In the case of 7-KChol and 5,6β-EChol, this transition shifts slightly toward higher surface pressures (~6–7 mN/m), indicating that the oxysterols stabilize the LE–LC coexistence region at low sterol concentrations. In mixed DPPC monolayers at $X_{sterol} = 0.3$, the LE–LC coexistence region is still observed for 7-KChol and 5,6β-EChol at ~4–5 mN/m but is not discernible for Chol. At $X_{sterol} \geq 0.5$ the LE–LC coexistence region is no longer observable in any of the mixed DPPC/sterol monolayers.

The variation of the monolayer compressibility modulus with sterol composition was also evaluated at surface pressures ranging from 3 to 40 mN/m (see Figure S2 in Supporting Information). With the addition of small amounts of sterols (i.e., $0 \leq X_{sterol} \leq 0.1$), C_s^{-1} decreases, especially in the surface pressure range from 20 to 40 mN/m. This lowering of the C_s^{-1} values in the presence of the sterols at low concentration has been reported previously and is the result of the sterols destabilizing the LC phase.[51] In the range of $X_{Chol} = 0.1–0.3$,

DOI: 10.1021/acs.langmuir.5b02539
Langmuir 2015, 31, 9859–9869

the compressibility modulus of the mixed DPPC/Chol monolayers remains practically unchanged; however, moving from X_{Chol} = 0.3 to 0.7, it increases almost linearly at all surface pressures. In contrast, in the same molar ratio range, only a small increase is observed in the mixed monolayers of 7-KChol and 5,6β-EChol, thus illustrating the lower interfacial rigidity of mixed DPPC/oxysterols monolayers. For example, in 7-KChol mixed monolayers, large compressibility moduli ($C_s^{-1} \geq 250$ mN/m) are only achieved for $X_{7\text{-KChol}}$ = 0.5 (C_s^{-1} = 272 mN/m), while with 5,6β-EChol, no such values are reached at any sterol composition. In comparison, for mixed DPPC/Chol monolayers, high compressibility modulus values are readily obtained with $X_{Chol} \geq 0.5$. The larger C_s^{-1} observed in the mixed DPPC/Chol monolayer is the result of Chol's ability to better order the alkyl chains of DPPC.

It is clear that the monolayer compressibility modulus is affected by the oxysterol type as 5,6β-EChol demonstrated the smallest values. As mentioned previously, this could be due to the molecular structure of the oxysterols as well as their average tilt in the DPPC monolayers. Previous atomistic MD simulations have shown that a difference in tilt exists between Chol and some of its derivatives and that it could be a major factor in the ordering effect of sterols on DPPC bilayers.[27,52] Smondyrev and Berkowitz studied the orientation of 6-ketocholestanol, an analogue of 7-KChol, in a DPPC bilayer and found it to be tilted (relative to the bilayer normal) with its ketone group oriented toward the aqueous phase, preferring to be hydrated rather than to be buried in the hydrophobic core of the alkyl chains. Because of the structural similarities between 6-ketocholestanol and 7-KChol, it is likely that 7-KChol must also be tilted and therefore closer to the air/water interface. In contrast, Aittoniemi and co-workers showed that the tilt of 3-ketocholesterol, another analogue of 7-KChol with a ketone group at position C3, remained unchanged relative to that of Chol. In their model, Chol was shown to have the smallest tilt (~20°) and to reside almost perpendicular to the bilayer plane, hence enabling it to have better ordering ability relative to its oxidized derivatives. More recently, a comprehensive study by Jungwirth and co-workers has shown that the position of the oxidation on Chol leads to different tilt angle distributions, with tail-oxidized sterols adopting nearly perpendicular orientation, whereas ring-oxidized ones like 7-KChol display a more pronounced tilt (~27°).[29] Because 5,6β-EChol has its oxidation on the steroid nucleus, it could also have a significant tilt relative to Chol and could explain its weaker ability to increase interfacial rigidity of DPPC monolayers; however, to the authors' knowledge, no comparable simulation on the tilt orientation of 5,6β-EChol in bilayers has so far been reported.

Excess Free Energy of Mixing of DPPC/Sterol Monolayers. The nonideality of the mixed DPPC/sterol monolayers was assessed, and the interactions between individual components were quantitatively analyzed by calculating the excess free energy of mixing (ΔG_{exc}) from the compression isotherms as a function of sterol composition (Figure 5A–C). Practically all investigated mixtures demonstrate nonideality ($\Delta G_{exc} < 0$) over the entire surface pressure range, indicating attractive DPPC–sterol interactions. Further analysis reveals that at lower surface pressures (3 and 10 mN/m) the most stable mixed DPPC/sterol monolayers exist at X_{sterol} = 0.5. However, at higher surface pressures (20, 30, and 40 mN/m), the minimum ΔG_{exc} shifts toward a monolayer composition richer in DPPC (X_{sterol} = 0.3). At this sterol composition and at a surface pressure of 40 mN/m, the excess free energy of mixing follows the order 7-KChol ≈ Chol > 5,6β-EChol. In other words, DPPC monolayers with 7-KChol and Chol are more thermodynamically stable based on achieving the smallest excess free energy values.

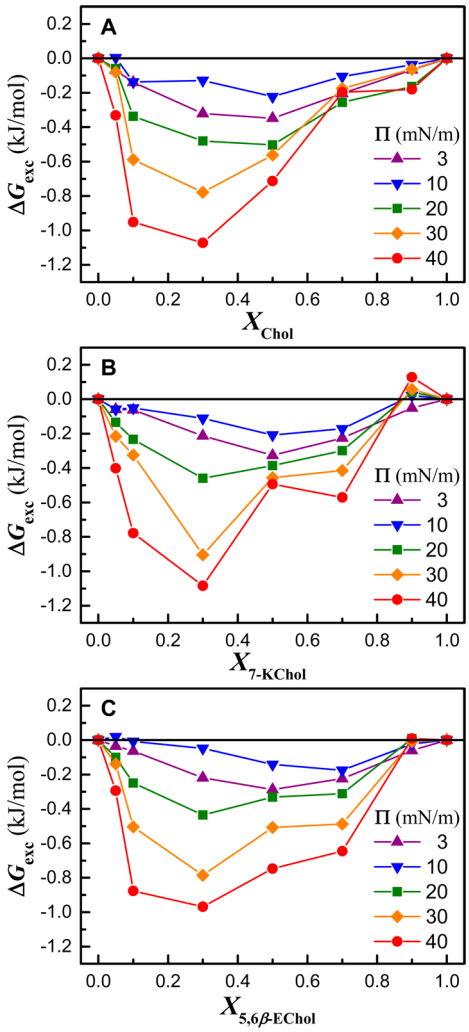

Figure 5. Variations of excess free energy of mixing with sterol composition for (A) Chol, (B) 7-KChol, and (C) 5,6β-EChol in binary mixtures with DPPC. The DPPC/5,6β-EChol mixture is slightly less stable relative to the other mixtures. Also note that the minimum in the excess free energy transitions with increasing surface pressure from X_{sterol} = 0.5 to 0.3 for all three sterols.

Because of its greater hydrophilicity compared to Chol, 7-KChol might be expected to have a low thermodynamic stability when mixed with DPPC as the presence of the ketone group in the hydrophobic environment of the DPPC alkyl chains would make DPPC/7-KChol interactions less favorable;[52] however, this was not observed. Instead, DPPC/5,6β-EChol mixed monolayers displayed the lowest thermodynamic stability. Not only does this oxysterol lack planarity on the steroid A–B rings, but its configuration also brings the epoxy moiety in closer proximity to the hydrophobic alkyl chains, thereby increasing steric effects.[21] Hence, the differences in the excess free energy of DPPC/oxysterol monolayers appear to be strongly correlated to the positioning of the oxygen moiety on the sterol ring relative to the DPPC alkyl chains.

Morphology of Pure DPPC and Sterol Monolayers. The domain morphology of pure monolayers was first investigated by BAM prior to mixed monolayer studies. Figure

DOI: 10.1021/acs.langmuir.5b02539
Langmuir 2015, 31, 9859–9869

6A shows BAM images of the pure DPPC monolayer. At large MMAs (>100 Å^2/molecule) and low surface pressures (~1

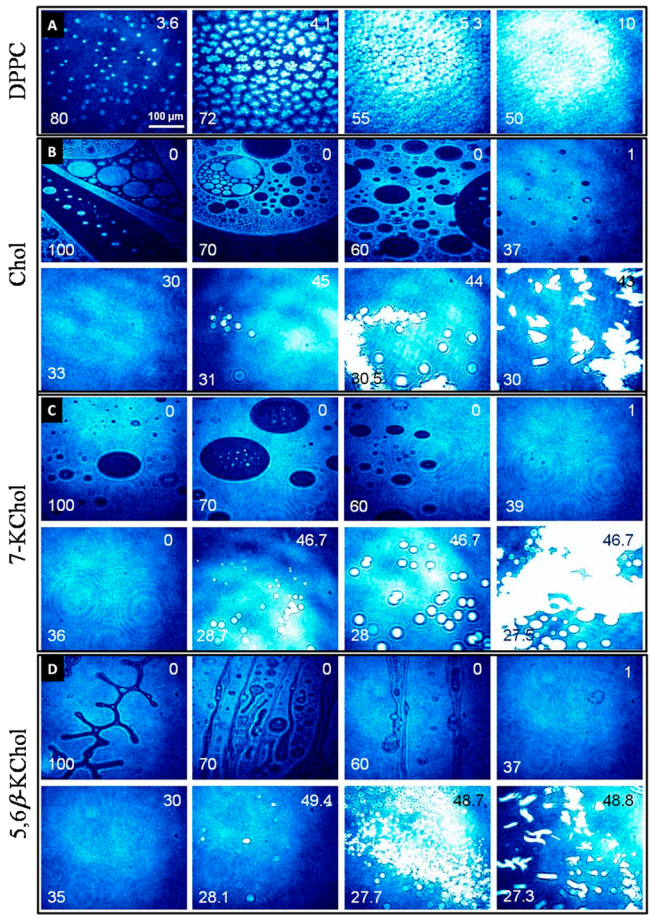

Figure 6. BAM images of pure (A) DPPC, (B) Chol, (C) 7-KChol, and (D) 5,6β-EChol monolayers at different stages of compression. Numbers in the lower left and upper right corners indicate the MMA and the surface pressure, respectively.

mN/m) the BAM image is homogeneous with very low reflectance (image not shown), which is indicative of the gas−liquid expanded (G−LE) phase. Once the LE−LC coexistence region is reached at ~3.6 mN/m, small bright irregular (likely multilobed but difficult to resolve with BAM) LC domains are observed, immersed in the darker LE phase. The phase segregation of DPPC into these two phases is the result of differences in alkyl chain ordering, as the LC phase is characterized by highly ordered alkyl chains, whereas in the LE phase, chains are disordered. At slightly higher surface pressures (~4 mN/m), larger multilobed LC domains can be more easily resolved. These changes in DPPC domain morphology are consistent with previously published fluorescence microscopy images obtained on DPPC monolayers.[31] The LC domains eventually grow in size along the LE−LC phase until they coalesce into one homogeneous condensed phase.

In the case of the Chol monolayer BAM images revealed that at large MMAs ($A \geq 70$ Å^2/molecule), circular- and stripe-like condensed domains coexist with the gas phase (Figure 6B). Upon further compression of the monolayer, most of these domains merge into a completely homogeneous condensed phase ($\Pi \sim 30$ mN/m). Approaching the collapse phase, small circular-like 3D crystalline Chol aggregates begin to emerge. Further compression leads to the clustering of these aggregates which are now larger in size and more numerous. However, following the drop in the surface pressure after collapse, the small aggregates appear to transition from a circular- to a rod-like shape.

In comparison to Chol, the 7-KChol monolayer shows almost no isolated condensed domains at large MMAs, but rather a largely condensed phase with few circular dark (lipid-poor) regions of different sizes scattered throughout, indicative of a less compact monolayer (Figure 6C). Further compression of the monolayer also resulted in a homogeneous condensed phase, although at a slightly larger MMA (39 Å^2/molecule) than Chol, consistent with the compression isotherm (Figure 2). At the collapse phase, similar to Chol, small circular-like 3D aggregates are observed followed by an increase in their size and number at higher surface pressures. However, unlike Chol, no change in the aggregate shape occurs with further compression. Instead, the 3D aggregates continued to increase in size and eventually became much larger than those of Chol. Much like the pure 7-KChol monolayer, very few condensed domains are seen at large MMAs in the 5,6β-EChol monolayer; instead, a quasi-condensed phase is observed with darker worm-like channels running across it (Figure 6D). At MMAs of 60−70 Å^2/molecule, these lipid-poor regions transformed into filiform and circular domains. Like Chol and 7-KChol, the collapse phase of 5,6β-EChol also shows the appearance of circular-like 3D aggregates, although in much smaller and in greater number. Further compression finally causes a shape transition into rod-like structures much like those of Chol.

The BAM images here confirm that the molecular structure of the sterols also has an impact on the domain morphology of pure monolayers, particularly in the collapse region. To explain these differences, previous studies determined that Chol can have two types of 3D collapse aggregates in the bulk monolayer: monohydrate and anhydrous, with the monohydrate being the most stable form in water.[53] GIXD experiments have further shown that the 3D aggregates of collapsed Chol monolayers are in fact trilayers consisting of a bilayer and a disordered Chol monolayer separated by one water layer.[54,55] This water layer is suggested to maintain a continuous hydrogen bonding channel between the hydroxyl groups of Chol molecules from the monolayer and bilayer. These interactions are believed to stabilize the crystal structure of the aggregates.[55] X-ray diffraction was also used to determine the hydrated crystal structure of 7-KChol.[56] Notable differences in the crystal structures of 7-KChol and Chol were found and traced back to the participation of the ketone group in the hydrogen-bonding network in addition to two hydroxyl groups from other 7-KChol molecules. This additional binding may disrupt the hydrogen-bonding channel that is associated with the Chol monohydrate. This is consistent with the BAM images of the sterol collapse phases, which show that the ketone group of 7-KChol has a greater impact on the shape of the 3D collapse aggregates than Chol (as well as 5,6β-EChol). Another interesting feature that is observed here is the relative size of the 7-KChol 3D collapse structures in comparison to those of Chol and 5,6β-EChol, which are on average 3−6 times larger, indicating more molecules per aggregation site. This increase in the aggregation size of 7-KChol is manifested by a significant increase in reflectance observed from the BAM images, suggesting the formation of multilayer structures that are thicker than those of the other two sterols. This observation

DOI: 10.1021/acs.langmuir.5b02539
Langmuir 2015, 31, 9859−9869

may be directly correlated to the different collapse mechanism seen in the isotherms.

Morphology of Mixed DPPC/Sterol Monolayers. The BAM images shown in Figure 7A correspond to DPPC/sterol monolayers with X_{sterol} = 0.05 at different stages of compression. With the addition of such a small amount of sterol, a change to the domain morphology is readily observable in the LE–LC phase (A = 60–70 Å^2/molecule; second and third columns in Figure 7A), where the irregularly shaped LC domains of the pure DPPC monolayer are replaced by smaller domains in the mixed monolayers. However, the shape of these domains is not easily discernible due to the available BAM resolution. Previous studies using epifluorescence microscopy, atomic force microscopy (AFM), and near-field scanning optical microscopy (NSOM) have shown that DPPC/Chol monolayers at similar Chol ratios consist of spiral-shaped LC domains with increased domain perimeter.[57−59] These studies suggest that Chol prefers to reside at the boundary between the condensed and fluid phases hence reducing the line tension.[60] This preference of Chol to partition to the perimeter of the domains also has been documented in molecular dynamics simulations, fluorescence microscopy, and AFM studies.[61,62] More recently, Zasadzinki and co-workers indicated that Chol may actually be "soluble" in the LC domains.[62] The LC domains in the LE–LC phase of the mixed DPPC/5,6β-EChol monolayer are larger, indicating that among the three sterols, 5,6β-EChol shows the least aptitude for the boundary. Because the oxysterols appear to have a greater affinity for the LE phase and a lesser ability to reduce line tension at the LE–LC phase boundary than Chol, this results in larger DPPC LC domains compared to Chol and more disordered alkyl chains in the LE phase and is consistent with the reduced rigidity of the oxysterols. The partitioning of oxysterols between the DPPC LE and LC phases and their effect on the LC domain number and size is illustrated schematically in Figure 8.

In DPPC/sterol monolayers with X_{sterol} = 0.3, the condensed domains surrounded by the LE phase usually found in the pure DPPC monolayer are no longer present (Figure 7B). At this molar ratio, Chol induces heterogeneity in the images in the low surface pressure regime. In contrast, BAM images of DPPC/oxysterol monolayers were quite homogeneous throughout the entire compression. The heterogeneity seen at

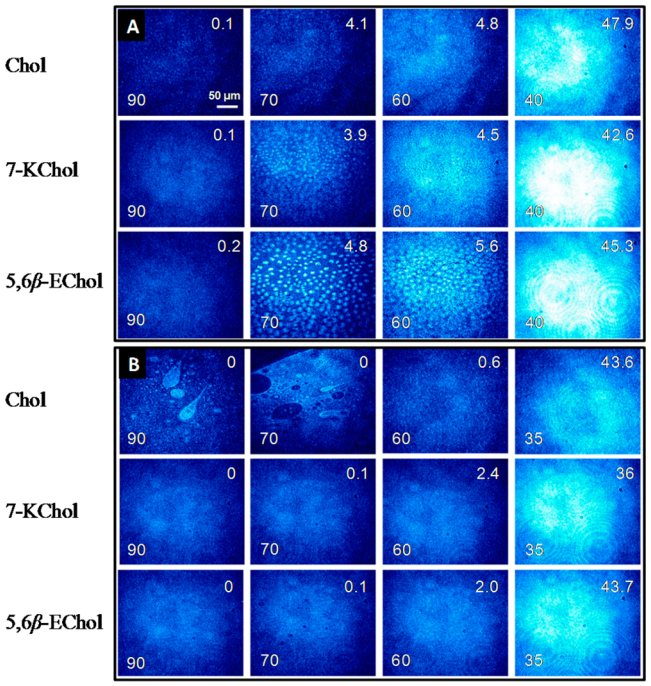

Figure 7. BAM images of mixed DPPC/sterol monolayers with (A) X_{sterol} = 0.05 and (B) X_{sterol} = 0.3 at different stages of compression. Numbers in the lower left and upper right corners indicate the MMA and the surface pressure, respectively.

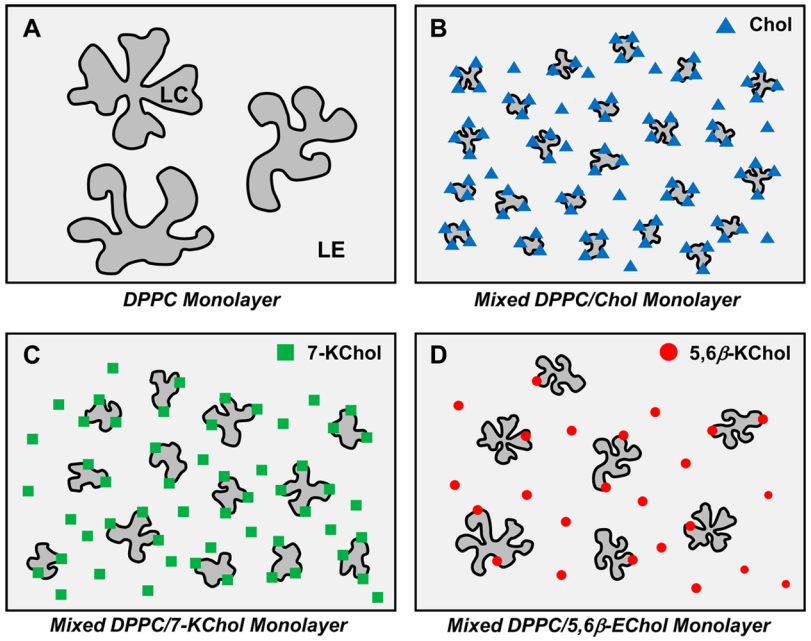

Figure 8. Schematic model of DPPC domain morphology in the LE–LC coexistence phase for (A) pure DPPC monolayer and for (B–D) DPPC monolayers mixed with Chol, 7-KChol, and 5,6β-Echol at X_{sterol} = 0.1. The LC domains in the LE–LC phase of mixed DPPC/oxysterol are larger due to the low affinity of the oxysterol for the phase boundary.

DOI: 10.1021/acs.langmuir.5b02539
Langmuir 2015, 31, 9859–9869

X_{Chol} = 0.3 was previously reported and was shown to be the result of three separate phases in coexistence with each other, with Chol-rich and Chol-poor domains.[59] Because a similar effect is not observed with the oxysterols suggests that they are not able to phase separate in the same way with DPPC.

CONCLUSION

This study assessed the effects of two ring-substituted oxysterols, 7-KChol and 5,6β-EChol, on the condensing effect, thermodynamic stability, interfacial rigidity, and domain morphology of DPPC monolayers for different surface pressures and sterol molar ratios. Analysis of the compression isotherm results for mixed DPPC/sterol monolayers showed that 7-KChol and 5,6β-EChol have a more limited condensing and ordering ability on DPPC than Chol, thus leaving DPPC monolayers with a much reduced interfacial rigidity. BAM images further revealed that in the LE−LC phase at low sterol concentration all three sterols interact with the DPPC domains by partitioning at the phase boundary; however, oxysterols are not as effective at fluidizing the LC phase relative to Chol as observed by the larger domain size. Differences in terms of condensing ability between 7-KChol and 5,6β-EChol could also be noted. In contrast to 7-KChol, the nonplanarity of the steroid nucleus in 5,6β-EChol causes the projection of the epoxy moiety out of its plane potentially enabling it to disrupt the DPPC alkyl chain ordering, thereby increasing instability in the monolayer. These results taken together lead to the conclusion that the molecular structure, sterol hydrophobicity character and tilt orientation which depend on the oxidation position on the steroid nucleus are likely responsible for the oxysterols lesser condensing ability, decreased interfacial rigidity, and increasing instability imparted to DPPC monolayers in comparison to Chol.

Future studies will focus on examining the influence of PC alkyl chain length on the magnitude of the condensing and ordering effects induced by each oxysterol for different chemical compositions. Depending on the chain length, the hydrophobic mismatch between PC alkyl chains and oxysterols could either counteract or reinforce the van der Waals interactions and therefore affect the overall stability of the mixed monolayers. Additionally, as shown by recent MD simulations,[29] the breadth and location of the angular tilt distribution of oxysterols relative to Chol depend largely on the oxidation position. However, so far, there have been very few experimental results to support this molecular picture. Further studies using surface-sensitive spectroscopic techniques such as infrared reflection−absorption spectroscopy (IRRAS) and vibrational sum-frequency generation (VSFG) spectroscopy applied to pure and mixed DPPC/sterol monolayers will enable to retrieve the orientational information about the oxysterols. Finally, as in real marine aerosols Chol will be present alongside oxysterols, it would be interesting to look at the synergistic/antagonistic interactions between these sterols and their ability to promote (or not) DPPC monolayer condensation in ternary mixtures. All these studies would provide a more complete understanding of lipid−sterol interactions and how these ultimately affect the surface reactivity and stability of the organic layer on marine aerosols.

With regards to implications of this work on atmospheric phenomena, Chol and its oxidation products are likely to be encountered in marine aerosol due to their prevalence in cellular membranes of marine organisms. Because of the lower hydrophobicity of the oxysterols relative to Chol, the interfacial rigidity of the lipid layer will be reduced, thereby changing the water evaporation characteristics of the aerosol. Also, the reflectance of the aerosol changes, correlated with disruption of the monolayer, therefore changing the surface refractive index, likely impacting the radiative properties of marine aerosols.

ASSOCIATED CONTENT

Supporting Information

The Supporting Information is available free of charge on the ACS Publications website at DOI: 10.1021/acs.langmuir.5b02539.

Plots of the variation of MMA and monolayer compressibility modulus as a function of sterol composition (PDF)

AUTHOR INFORMATION

Corresponding Author

*E-mail allen@chemistry.ohio-state.edu; Ph (614) 292-4707 (H.C.A.).

Notes

The authors declare no competing financial interest.

ACKNOWLEDGMENTS

The authors acknowledge NSF-CHE (1111762) for funding this work.

REFERENCES

(1) O'Dowd, C. D.; De Leeuw, G. Marine aerosol production: A review of the current knowledge. *Philos. Trans. R. Soc., A* **2007**, *365*, 1753−1774.

(2) Boucher, O.; Randall, D.; Artaxo, P.; Bretherton, C.; Feingold, G.; Forster, P.; Kerminen, V.-M.; Kondo, Y.; Liao, H.; Lohmann, U.; Rasch, P.; Satheesh, S. K.; Sherwood, S.; Stevens, B.; Zhang, X. Y. Clouds and aerosols. In *Climate Change 2013: The Physical Science Basis. Contribution of Working Group I to The Fifth Assessment Report of The Intergovernmental Panel on Climate Change*; Cambridge University Press: Cambridge, UK, 2013; pp 571−657.

(3) Lewis, E. R.; Schwartz, S. E. *Sea Salt Aerosol Production: Mechanisms, Methods, Measurements, and Models - A Critical Review*; American Geophysical Union: Washington, DC, 2004.

(4) Rinaldi, M.; Decesari, S.; Finessi, E.; Giulianelli, L.; Carbone, C.; Fuzzi, S.; O'Dowd, C. D.; Ceburnis, D.; Facchini, M. C. Primary and secondary organic marine aerosol and oceanic biological activity: Recent results and new perspectives for future studies. *Adv. Meteorology* **2010**, *2010*, 310682.

(5) Cunliffe, M.; Engel, A.; Frka, S.; Gašparović, B.; Guitart, C.; Murrell, J. C.; Salter, M.; Stolle, C.; Upstill-Goddard, R.; Wurl, O. Sea surface microlayers: A unified physicochemical and biological perspective of the air−ocean interface. *Prog. Oceanogr.* **2013**, *109*, 104−116.

(6) O'Dowd, C. D.; Facchini, M. C.; Cavalli, F.; Ceburnis, D.; Mircea, M.; Decesari, S.; Fuzzi, S.; Yoon, Y. J.; Putaud, J. P. Biogenically driven organic contribution to marine aerosol. *Nature* **2004**, *431*, 676−680.

(7) Suzumura, M. Phospholipids in marine environments: A review. *Talanta* **2005**, *66*, 422−434.

(8) Brandsma, J.; Hopmans, E. C.; Philippart, C. J. M.; Veldhuis, M. J. W.; Schouten, S.; Sinninghe Damsté, J. S. Low temporal variation in the intact polar lipid composition of North Sea coastal marine water reveals limited chemotaxonomic value. *Biogeosciences* **2012**, *9*, 1073−1084.

(9) Rontani, J.-F.; Charrière, B.; Sempéré, R.; Doxaran, D.; Vaultier, F.; Vonk, J. E.; Volkman, J. K. Degradation of sterols and terrigenous organic matter in waters of the Mackenzie Shelf, Canadian Arctic. *Org. Geochem.* **2014**, *75*, 61−73.

DOI: 10.1021/acs.langmuir.5b02539
Langmuir 2015, 31, 9859−9869

(10) Barbier, M.; Tusseau, D.; Marty, J. C.; Saliot, A. Sterols in aerosols, surface microlayer and subsurface water in the northeastern tropical atlantic. *Oceanol. Acta* **1981**, *4*, 77−84.
(11) Volkman, J. K. A review of sterol markers for marine and terrigenous organic matter. *Org. Geochem.* **1986**, *9*, 83−99.
(12) Tervahattu, H.; Hartonen, K.; Kerminen, V. M.; Kupiainen, K.; Aarnio, P.; Koskentalo, T.; Tuck, A. F.; Vaida, V. New evidence of an organic layer on marine aerosols. *J. Geophys. Res.* **2002**, *107*, 2000JD000282.
(13) Gill, P. S.; Graedel, T. E.; Weschler, C. J. Organic films on atmospheric aerosol-pariticles, fog, droplets, cloud droplets, raindrops and snowflakes. *Rev. Geophys.* **1983**, *21*, 903−920.
(14) Donaldson, D. J.; Vaida, V. The influence of organic films at the air-aqueous boundary on atmospheric processes. *Chem. Rev.* **2006**, *106*, 1445−1461.
(15) Ellison, G. B.; Tuck, A. F.; Vaida, V. Atmospheric processing of organic aerosols. *J. Geophys. Res.* **1999**, *104*, 11633−11641.
(16) Ohvo-Rekilä, H.; Ramstedt, B.; Leppimäki, P.; Slotte, J. P. Cholesterol interactions with phospholipids in membranes. *Prog. Lipid Res.* **2002**, *41*, 66−97.
(17) Stottrup, B. L.; Keller, S. L. Phase behavior of lipid monolayers containing DPPC and cholesterol analogs. *Biophys. J.* **2006**, *90*, 3176−3183.
(18) Wydro, P.; Knapczyk, S.; Łapczyńska, M. Variations in the condensing effect of cholesterol on saturated versus unsaturated phosphatidylcholines at low and high sterol concentration. *Langmuir* **2011**, *27*, 5433−5444.
(19) Iuliano, L. Pathways of cholesterol oxidation via non-enzymatic mechanisms. *Chem. Phys. Lipids* **2011**, *164*, 457−468.
(20) Björkhem, I.; Diczfalusy, U. Oxysterols - Friends, foes, or just fellow passengers? *Arterioscler., Thromb., Vasc. Biol.* **2002**, *22*, 734−742.
(21) Massey, J. B.; Pownall, H. J. Structures of biologically active oxysterols determine their differential effects on phospholipid membranes. *Biochemistry* **2006**, *45*, 10747−10758.
(22) McNeill, V. F.; Sareen, N.; Schwier, A. N. Surface-Active Organics in Atmospheric Aerosols. In *Atmospheric and Aerosol Chemistry*; McNeill, V. F., Ariya, P. A., Eds.; Springer: New York, 2014; Vol. *339*, pp 201−259.
(23) Wilke, N. Lipid Monolayers at the Air-Water Interface: A Tool for Understanding Electrostatic Interactions and Rheology in Biomembranes. In *Advances in Planar Lipid Bilayers and Liposomes*; Iglic, A., Kulkarni, C. V., Eds.; Elsevier: Amsterdam, 2014; pp 51−81.
(24) Bach, D.; Epand, R. F.; Epand, R. M.; Miller, I. R.; Wachtel, E. The oxidized form of cholesterol 3β-hydroxy-5-oxo-5,6-secocholestan-6-al induces structural and thermotropic changes in phospholipid membranes. *Chem. Phys. Lipids* **2009**, *161*, 95−102.
(25) Kamel, A. M.; Felmeist, A.; Weiner, N. D. Surface pressure-surface area characteristics of a series of autoxidation products of cholesterol. *Lipid Res.* **1971**, *12*, 155−159.
(26) Ma, S.; Li, H.; Tian, K.; Ye, S.; Luo, Y. In situ and real-time SFG measurements revealing organization and transport of cholesterol analogue 6-ketocholestanol in a cell membrane. *J. Phys. Chem. Lett.* **2014**, *5*, 419−424.
(27) Aittoniemi, J.; Róg, T.; Niemelä, P.; Pasenkiewicz-Gierula, M.; Karttunen, M.; Vattulainen, I. Tilt: Major factor in sterols' ordering capability in membranes. *J. Phys. Chem. B* **2006**, *110*, 25562−25564.
(28) Kamal, M. A.; Raghunathan, V. A. Effect of ring-substituted oxysterols on the phase behavior of dipalmitoylphosphatidylcholine membranes. *Eur. Biophys. J.* **2012**, *41*, 891−900.
(29) Kulig, W.; Olzynska, A.; Jurkiewicz, P.; Kantola, A. M.; Komulainen, S.; Manna, M.; Pourmousa, M.; Vazdar, M.; Cwiklik, L.; Róg, T.; Khelashvili, G.; Harries, D.; Telkki, V.-V.; Hof, M.; Vattulainen, I.; Jungwirth, P. Cholesterol under oxidative stress-How lipid membranes sense oxidation as cholesterol is being replaced by oxysterols. *Free Radical Biol. Med.* **2015**, *84*, 30−41.
(30) Mintzer, E.; Charles, G.; Gordon, S. Interaction of two oxysterols, 7-ketocholesterol and 25-hydroxycholesterol, with phosphatidylcholine and sphingomyelin in model membranes. *Chem. Phys. Lipids* **2010**, *163*, 586−593.
(31) Klopfer, K. J.; Vanderlick, T. K. Isotherms of dipalmitoylphosphatidylcholine (DPPC) monolayers: Features revealed and features obscured. *J. Colloid Interface Sci.* **1996**, *182*, 220−229.
(32) Chattoraj, D. K.; Birdi, K. S. *Adsorption and the Gibbs Surface Excess*; Springer: New York, 1984.
(33) Benvegnu, D. J.; McConnell, H. M. Surface dipole densities in lipid monolayers. *J. Phys. Chem.* **1993**, *97*, 6686−6691.
(34) Li, X. M.; Momsen, M. M.; Smaby, J. M.; Brockman, H. L.; Brown, R. E. Cholesterol decreases the interfacial elasticity and detergent solubility of sphingomyelins. *Biochemistry* **2001**, *40*, 5954−5963.
(35) Dynarowicz-Latka, P.; Kita, K. Molecular interaction in mixed monolayers at the air/water interface. *Adv. Colloid Interface Sci.* **1999**, *79*, 1−17.
(36) Chapman, D.; Owens, N. F.; Phillips, M. C.; Walker, D. A. Mixed monolayers of phospholipids and cholesterol. *Biochim. Biophys. Acta, Biomembr.* **1969**, *183*, 458−465.
(37) Seoane, R.; Miñones, J.; Conde, O.; Miñones, J., Jr.; Casas, M.; Iribarnegaray, E. Thermodynamic and Brewster angle microscopy studies of fatty acid/cholesterol mixtures at the air/water interface. *J. Phys. Chem. B* **2000**, *104*, 7735−7744.
(38) Slotte, J. P.; Jungner, M.; Vilchèze, C.; Bittman, R. Effect of sterol side-chain structure on sterol-phosphatidylcholine interactions in monolayers and small unilamellar vesicles. *Biochim. Biophys. Acta, Biomembr.* **1994**, *1190*, 435−443.
(39) Theunissen, J. J. H.; Jackson, R. L.; Kempen, H. J. M.; Demel, R. A. Membrane properties of oxysterols interfacial orientation, influence on membrane permeability and redistribution between membranes. *Biochim. Biophys. Acta, Biomembr.* **1986**, *860*, 66−74.
(40) Snik, A. F. M.; Kruger, A. J.; Joos, P. Dynamical behavior of monolayers of dipalmitoyl lecithin and cholesterol. *J. Colloid Interface Sci.* **1978**, *66*, 435−439.
(41) McConlogue, C. W.; Malamud, D.; Vanderlick, T. K. Interaction of DPPC monolayers with soluble surfactants: electrostatic effects of membrane perturbants. *Biochim. Biophys. Acta, Biomembr.* **1998**, *1372*, 124−134.
(42) Miñones, J., Jr.; Rodriguez Patino, J. M.; Conde, O.; Carrera, C.; Seoane, R. The effect of polar groups on structural characteristics of phospholipid monolayers spread at the air-water interface. *Colloids Surf., A* **2002**, *203*, 273−286.
(43) Duncan, S. L.; Larson, R. G. Comparing experimental and simulated pressure-area isotherms for DPPC. *Biophys. J.* **2008**, *94*, 2965−2986.
(44) Hu, Y. F.; Lee, K. Y. C.; Israelachvili, J. Sealed minitrough for microscopy and long-term stability studies of Langmuir monolayers. *Langmuir* **2003**, *19*, 100−104.
(45) Su, Y.; Li, Q.; Chen, L.; Yu, Z. Condensation effect of cholesterol, stigmasterol, and sitosterol on dipalmitoylphosphatidylcholine in molecular monolayers. *Colloids Surf., A* **2007**, *293*, 123−129.
(46) Dynarowicz-Latka, P.; Hac-Wydro, K. Interactions between phosphatidylcholines and cholesterol in monolayers at the air/water interface. *Colloids Surf., B* **2004**, *37*, 21−25.
(47) McConnell, H. M.; Radhakrishnan, A. Condensed complexes of cholesterol and phospholipids. *Biochim. Biophys. Acta, Biomembr.* **2003**, *1610*, 159−173.
(48) de Meyer, F.; Smit, B. Effect of cholesterol on the structure of a phospholipid bilayer. *Proc. Natl. Acad. Sci. U. S. A.* **2009**, *106*, 3654−3658.
(49) Davies, J. T.; Rideal, E. K. *Interfacial Phenomena*, 2nd ed.; Academic Press: New York, 1963.
(50) Sabatini, K.; Mattila, J.-P.; Kinnunen, P. K. J. Interfacial behavior of cholesterol, ergosterol, and lanosterol in mixtures with DPPC and DMPC. *Biophys. J.* **2008**, *95*, 2340−2355.
(51) Li, X. M.; Momsen, M. M.; Brockman, H. L.; Brown, R. E. Sterol structure and sphingomyelin acyl chain length modulate lateral packing elasticity and detergent solubility in model membranes. *Biophys. J.* **2003**, *85*, 3788−3801.

DOI: 10.1021/acs.langmuir.5b02539
Langmuir 2015, 31, 9859−9869

(52) Smondyrev, A. M.; Berkowitz, M. L. Effects of oxygenated sterol on phospholipid bilayer properties: a molecular dynamics simulation. *Chem. Phys. Lipids* **2001**, *112*, 31−39.
(53) Loomis, C. R.; Shipley, G. G.; Small, D. M. Phase behavior of hydrated cholesterol. *J. Lipid Res.* **1979**, *20*, 525−535.
(54) Rapaport, H.; Kuzmenko, I.; Lafont, S.; Kjaer, K.; Howes, P. B.; Als-Nielsen, J.; Lahav, M.; Leiserowitz, L. Cholesterol monohydrate nucleation in ultrathin films on water. *Biophys. J.* **2001**, *81*, 2729−2736.
(55) Craven, B. M. Crystal structure of cholesterol monohydrate. *Nature* **1976**, *260*, 727−729.
(56) McCourt, M. P.; Ashraf, K.; Miller, R.; Weeks, C. M.; Li, N. Y.; Pangborn, W.; Dorset, D. L. X-ray crystal structure of cytotoxic oxidized cholesterols: 7-ketocholesterol and 25-hydroxycholesterol. *J. Lipid Res.* **1997**, *38*, 1014−1021.
(57) Weis, R. M.; McConnell, H. M. Cholesterol stabilizes the crystal liquid interface in phospholipid monolayers. *J. Phys. Chem.* **1985**, *89*, 4453−4459.
(58) Worthman, L. A. D.; Nag, K.; Davis, P. J.; Keough, K. M. W. Cholesterol in condensed and fluid phosphatidylcholine monolayers studied by epifluorescence microscopy. *Biophys. J.* **1997**, *72*, 2569−2580.
(59) Yuan, C.; Johnston, L. J. Phase evolution in cholesterol/DPPC monolayers: atomic force microscopy and near field scanning optical microscopy studies. *J. Microsc.* **2002**, *205*, 136−146.
(60) McConnell, H. M. Structures and transitions in lipid monolayers at the air-water interface. *Annu. Rev. Phys. Chem.* **1991**, *42*, 171−195.
(61) Duncan, S. L.; Dalal, I. S.; Larson, R. G. Molecular dynamics simulation of phase transitions in model lung surfactant monolayers. *Biochim. Biophys. Acta, Biomembr.* **2011**, *1808*, 2450−2465.
(62) Kim, K.; Choi, S. Q.; Zell, Z. A.; Squires, T. M.; Zasadzinski, J. A. Effect of cholesterol nanodomains on monolayer morphology and dynamics. *Proc. Natl. Acad. Sci. U. S. A.* **2013**, *110*, E3054−E3060.

DOI: 10.1021/acs.langmuir.5b02539
Langmuir 2015, 31, 9859−9869